NRL FR-7649

Reflection of Internal Gravity Waves by a Layered Density Anomaly

Richard P. Mied
John P. Dugan

December 21, 1973

Naval Research Laboratory
Washington D.C. 20362

SECURITY CLASSIFICATION OF THIS PAGE *(When Data Entered)*

REPORT DOCUMENTATION PAGE

READ INSTRUCTIONS BEFORE COMPLETING FORM

1. REPORT NUMBER: NRL Report 7649	2. GOVT ACCESSION NO.
3. RECIPIENT'S CATALOG NUMBER	
4. TITLE *(and Subtitle)*: REFLECTION OF INTERNAL GRAVITY WAVES BY A LAYERED DENSITY ANOMALY	5. TYPE OF REPORT & PERIOD COVERED: Final Report
6. PERFORMING ORG. REPORT NUMBER	
7. AUTHOR(s): Richard P. Mied and John P. Dugan	8. CONTRACT OR GRANT NUMBER(s)
9. PERFORMING ORGANIZATION NAME AND ADDRESS: Naval Research Laboratory, Washington, D.C. 20375	10. PROGRAM ELEMENT, PROJECT, TASK AREA & WORK UNIT NUMBERS: 83K03-11, WF-11-125-703
11. CONTROLLING OFFICE NAME AND ADDRESS: Department of the Navy, Naval Air Systems Command, Washington, D.C. 20361	12. REPORT DATE: December 21, 1973
	13. NUMBER OF PAGES: 31
14. MONITORING AGENCY NAME & ADDRESS*(if different from Controlling Office)*	15. SECURITY CLASS. *(of this report)*: Unclassified
	15a. DECLASSIFICATION/DOWNGRADING SCHEDULE

16. DISTRIBUTION STATEMENT *(of this Report)*

Approved for public release; distribution unlimited.

17. DISTRIBUTION STATEMENT *(of the abstract entered in Block 20, if different from Report)*

18. SUPPLEMENTARY NOTES

19. KEY WORDS *(Continue on reverse side if necessary and identify by block number)*

Internal gravity waves
Internal wave reflections
Pycnocline

20. ABSTRACT *(Continue on reverse side if necessary and identify by block number)*

Exact solutions are obtained for internal gravity waves incident upon a layered density anomaly embedded in a stably stratified fluid with otherwise constant Brunt-Väisälä frequency. Here, the Brunt-Väisälä frequency is composed of the sum of a constant, a bump (the square of a hyperbolic secant), and a transition region (a hyperbolic tangent). The reflection coefficient is a complicated function of the horizontal and vertical wave numbers, the parameters related to the Brunt-Väisälä profile, and of the angle theta which the phase speed makes with the horizontal far

(Continues)

DD FORM 1 JAN 73 1473 EDITION OF 1 NOV 65 IS OBSOLETE
S/N 0102-014-6601

SECURITY CLASSIFICATION OF THIS PAGE *(When Data Entered)*

20. (Continued)

from the anomaly. It is found that all wave energy is transmitted through the anomalous layer for vertically propagating waves and all is reflected for horizontally propagating ones, regardless of the dimensions of the anomaly or the wavelength of the incoming wave. Further, there can exist for some stratification conditions certain other directions of propagation for which the energy is totally transmitted. The transmission "windows" are seen to accumulate—in still more specialized cases—about the point theta = 90°. The reflection coefficient in the case of a stable density step in the profile is examined in the limit of vanishing step thickness.

CONTENTS

REFLECTION OF INTERNAL GRAVITY WAVES BY A LAYERED DENSITY ANOMALY

INTRODUCTION

The characteristics of the propagation of internal gravity waves in the ocean, either upward from the bottom or downward from the region of the surface, is of interest to oceanographers because of the implications to the total energy budget of the internal wave field. The ways by which these internal waves may be generated are numerous. Internal lee waves, for example, can be generated by current flow over bottom topography (1-3). The fate of these disturbances after they are generated depends upon the environment through which they travel. The absorption of the wave energy by critical layers has recently been of interest in this context (4, 5), but the reflection of waves by current shear or anomalies in the density profile has received somewhat less attention. Perhaps the simplest situation of physical interest in this regard is the propagation of a train of plane waves upward through a fluid which has an exponential dependence of density upon height. This plane wave will propagate without change in amplitude or direction (to the Boussinesq approximation) unless it encounters a density or shear anomaly. Layered regions like the thermocline change the propagation conditions, and part of the wave energy can, in principle, be reflected back toward its region of generation. This reflection problem has been considered in special cases by Hines and Reddy (6) and Barcilon et al. (7). In the former work, the density stratification is modeled with a series of strata, each of which are at a constant temperature. Because the density structures modeled are typical atmospheric soundings, the dependence of the reflection coefficient on the physical parameters (scale heights and density differences) is not easily discerned. In the latter paper, the properties of the medium are presumed to change slowly over a distance much greater than a vertical wavelength. Superimposed on this "slow" variation is a smaller, wave-scale variation. This fine structure can cause the reflection of a significant portion of the incident wave energy.

In this report, we consider the interaction of a plane internal wave train with a diffuse layer embedded in a density profile possessing an otherwise exponential dependence on height. The density structure is assumed to be of the form

$$\overline{\rho}(z) = \rho_0 \exp\left(\Delta z + \epsilon \tanh \sigma z + \epsilon_1 \ell n \cosh \sigma z\right) \qquad -\infty < z < \infty \tag{1}$$

where z increases positively downward (see Fig. 1). The case of a thin layer is obtained in the limit $\sigma \to \infty$. The analysis is similar to, but is an *expanded and corrected* form of, that of Epstein (8) for an analogous reflection problem in electromagnetic wave propagation theory.

The derived results are of physical significance in the case of the ocean, as the thermocline shapes discussed here bear at least a qualitative resemblance to those observed in the ocean. For example, Iselin (9) shows a distribution of Brunt-Väisälä frequency which is very much like Eq. (1) with $\epsilon \neq 0$, $\epsilon_1 = 0$ (see Fig. 2a). Just as significant, however,

Manuscript submitted August 24, 1973.

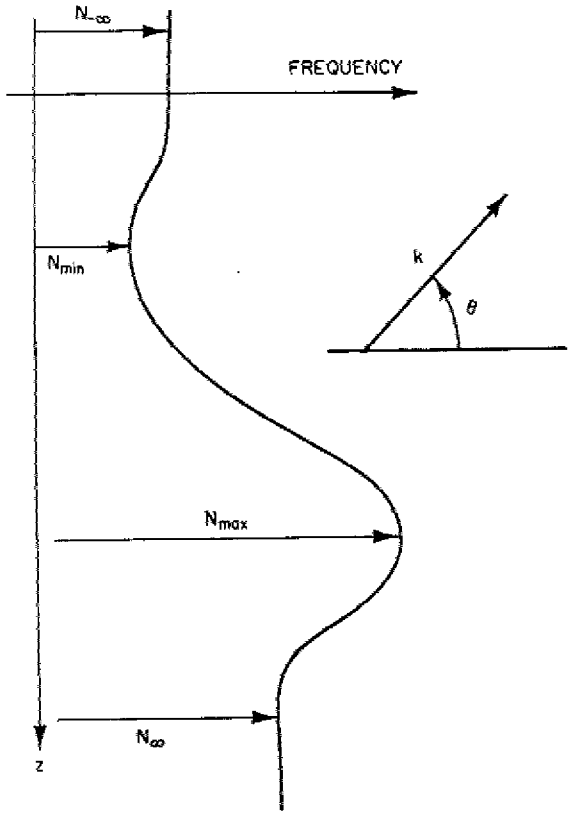

Fig. 1—An arbitrary Brunt-Väisälä frequency $N(z)$ profile as a function of height z.

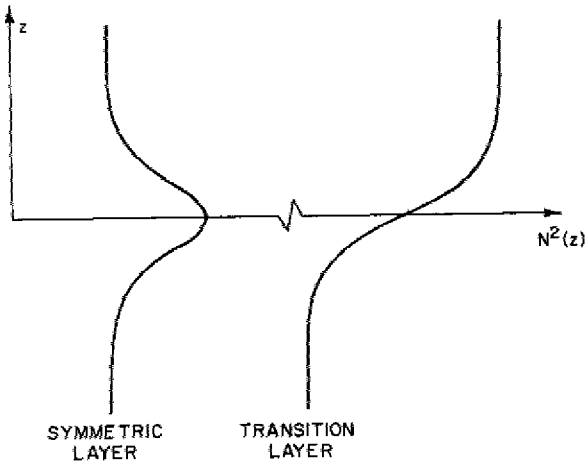

Fig. 2—(a) the symmetric profile ($\epsilon \neq 0$, $\epsilon_1 = 0$) and (b) the transition profile ($\epsilon = 0$, $\epsilon_1 \neq 0$). $N^2 = N^2(z)$.

may be the occurrence of steplike structures in the seasonal thermocline. Woods (10) reports an instance of the actual formation of this type of stepped structure resulting from the breaking of internal wavelets generated as a result of the instability to shear between layers of relatively homogeneous fluid masses, each possessing a different density. Phillips (11) and Orlanski and Bryan (12) argue that instabilities in the internal waves present are chiefly responsible for this stepped thermocline structure. Thermoclines resembling the form given by Eq. (1) and the sharp thermocline corresponding to $\sigma \to \infty$ in the same equation are therefore known to occur in the open ocean. It is of interest, then, to examine the internal wave propagation through, and energy reflection by, density distributions of this general form.

In the second section, we will present exact solutions for the transmitted and reflected waves obtained when a wave train is incident on a density anomaly possessing the form given by Eq. (1). The third section gives the expression for the reflection coefficient for a symmetrical layer ($\epsilon \neq 0$, $\epsilon_1 = 0$) and for a transitional layer ($\epsilon = 0$, $\epsilon_1 \neq 0$) between two regions having different Brunt-Väisälä frequencies. In each case the reflection coefficient has a deceptively simple appearance. It is actually a complicated function of the physical parameters, and even a small density anomaly can cause a significant reflection of waves traveling at a shallow angle to the horizontal.

The analysis involves an analytic continuation of the proper transmitted wave solution into the solutions which represent the incident and reflected waves. This analytic continuation formula is a classical one that exists only because the equation governing the dependence of the vertical velocity on the vertical coordinate can be transformed into Gauss' hypergeometric equation. Corresponding formulae generally do not exist for arbitrary density anomalies; but, the presentation of the work in this report allows one to vary density differences, the scale height of the anomaly, the vertical wave number, and the angle of incidence of the incoming wave in order to determine their individual effects upon the reflection coefficient. Because of the scarcity of such general forms for the reflection coefficient, a numerical technique that can be used in lieu of an analytic continuation for arbitrary Brunt-Väisälä distributions is presented in an appendix. The results of the numerical method are compared with the analytic results. The agreement is very good, and it is concluded that the numerical technique can be used in treating internal wave reflection from stability frequency profiles of arbitrary configuration.

THE REFLECTION PROBLEM

General Discussion

The equation governing two-dimensional, small-amplitude motions of an inviscid, density-stratified fluid about its equilibrium position is given (to the Boussinesq approximation) by Phillips (11) as

$$\frac{\partial^2}{\partial t^2}\left(\frac{\partial^2 w}{\partial x^2} + \frac{\partial^2 w}{\partial z^2}\right) + N^2(z)\,\frac{\partial^2 w}{\partial x^2} = 0, \tag{2}$$

where w is the vertical velocity component and $N^2(z)$ is the Brunt-Väisälä frequency defined by

$$N^2(z) = \frac{g}{\rho}\,\frac{d\bar{\rho}}{dz}\,. \tag{3}$$

The dimension z is taken to be increasing vertically downward, and the horizontal coordinate x is taken to be increasing positively to the right. The density of the fluid in its quiescent state is $\overline{\rho}(z)$, and the effects of diffusion and rotation have been neglected. If it is assumed that an internal gravity wave of frequency ω (less than the maximum over z of $N(z)$) and horizontal wave number k passes through the fluid, the velocity may be reduced by the substitution

$$w(x, z, t) = \phi(z)e^{i(kx-\omega t)}, \tag{4}$$

so that Eq. (2) reduces to

$$\phi_{zz} + \left[\frac{N^2(z)}{\omega^2} - 1\right] k^2\phi = 0. \tag{5}$$

We are particularly interested in fluids having density profiles of the form shown in Fig. 1. For simplicity, it is assumed that the Brunt-Väisälä frequency is constant outside of a layer, although the stability frequency in the region above the layer may in general be different from that below the layer. The density has a well-defined maximum and/or minimum value. Further, these extrema may or may not be in the anomalous layer. We remark that, for the ensuing analysis to be valid, the Brunt-Väisälä frequency outside the anomalous region need not be constant. It must satisfy only the weaker condition that it vary slowly enough over a vertical wavelength of the internal wave so that the WKB approximation is valid.

We are interested in wavelike solutions of Eq. (5), but it is well known that the equation has no such nontrivial solution that is regular at infinity if $\omega > N_{max}$. Thus, internal waves will propagate *only* if $\omega < N_{max}$. Moreover, there are two distinct types of wave solutions for this allowable frequency range. If the wave frequency ω is less than N_{max}, but everywhere greater than the Brunt-Väisälä frequency outside a bounded region surrounding the point where $N = N_{max}$, Eq. (5) allows nontrivial solutions for certain distinct combinations of the frequency and horizontal wave numbers; these solutions vanish far away from the anomalous region. In other words, this is a classical waveguide solution in which there is a discrete spectrum of trapped modes that propagate along the density anomaly. The greater of the two numbers N_∞ and $N_{-\infty}$ constitutes a lower cutoff frequency for these modes, so only a finite number of modes with the same wave number can propagate without attenuation.

The governing Eq. (5) also has a continuous spectrum of solutions in the frequency range $\omega < \max\{N_\infty, N_{-\infty}\}$. A plane wave of arbitrary frequency and wave number can propagate in the upper or lower region provided the wave frequency is less than the local Brunt-Väisälä frequency.

The problem of interest here is to determine what effect the anomalous layer has on a plane internal wave that is propagating upward in, say, the lower layer. To be explicit, we assume that a wave of frequency ω with horizontal wave number k is traveling upward through the lower fluid at angle θ to the horizontal. (The angle θ actually is fixed by the relation $\omega = N_\infty \cos\theta$ which is a result of Eq. (5) in the case of a plane wave at $z = +\infty$.) The wave enters the anomalous layer, and its amplitude and phase are changed as it propagates through the layer. As a result of the changing waveform, some of the wave energy is reflected back down into the lower layer and the remainder, if any, is transmitted upward into the upper layer. The exception involving the IF is foreseen because

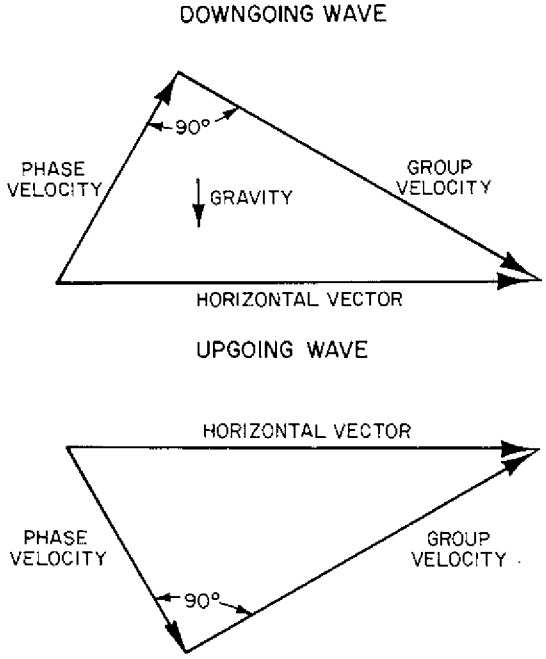

Fig. 3—The relation of the phase and group velocity vectors for internal waves in a stably stratified fluid.

of the case in which the wave frequency is greater than the Brunt-Väisälä frequency in the upper layer. This does not allow propagation there, and we will see that this causes total reflection of the wave.

The direction of energy propagation is not the direction of phase propagation in internal waves, so care must be exercised in specifying the direction of the phase velocity of the incoming wave. Phillips (11) discusses this matter in detail, and the relation of the group velocity to the phase velocity is shown in Fig. 3. The terminology used here is that an upward or downward propagating wave is one for which the direction of energy propagation (or group velocity) is upward or downward.

Solution of Governing Equation

The reflection problem with an arbitrary density profile and vertical wavelengths comparable to the thermocline scale height is, in general, analytically intractable; so, a particular distribution of stability frequency is chosen that exhibits the main features of the reflection phenomenon. The Brunt-Väisälä frequency obtained from Eqs. (1) and (3) is illustrated in Fig. 2 for the two cases $\epsilon \neq 0$, $\epsilon_1 = 0$ and $\epsilon = 0$, $\epsilon_1 \neq 0$. As may be seen, the former case has a stability frequency profile symmetric about depth $z = 0$. If $\epsilon > 0$, the fluid in the anomalous layer is more stable than that of its surroundings; if $\epsilon < 0$, however, the fluid in the layer is relatively homogeneous and consequently not as stable. The value of ϵ cannot be so negative that the stability frequency is negative *in toto* anywhere, since such a situation would be statically unstable. In the second case ($\epsilon = 0$, $\epsilon_1 \neq 0$), the anomalous layer is really a transition region between two layers of constant but different Brunt-Väisälä frequencies. If $\epsilon_1 > 0$, the transition in the

direction of primary waves (incident from below) is from more stable to less stable fluid. The opposite is the case for $\epsilon_1 < 0$; and again, we require that the magnitude of ϵ_1 be bounded so that the Brunt-Väisälä frequency is nonnegative everywhere.

The differential equation, Eq. (5), with the profile (1), is

$$\phi_{zz} + k^2\left\{\omega^{-2}g[\Delta + \epsilon\sigma \operatorname{sech}^2 \sigma z + \epsilon_1 \sigma \tanh \sigma z] - 1\right\}\phi = 0. \qquad (6)$$

This equation reduces to

$$\phi_{zz} + k^2\left\{\omega^{-2}g(\Delta + \epsilon_1\sigma) - 1\right\}\phi = 0 \qquad (7)$$

in the limit of large positive z (the lower propagation zone), and to

$$\phi_{zz} + k^2\left\{\omega^{-2}g(\Delta - \epsilon_1\sigma) - 1\right\}\phi = 0 \qquad (8)$$

in the limit of large negative z (the upper zone into which the transmitted wave propagates). In these regions, the equations allow the solutions

$$\phi \sim \exp\left\{\pm ik[\omega^{-2}g(\Delta + \epsilon_1\sigma) - 1]^{1/2}z\right\} \qquad (9)$$

for $z \to +\infty$ and

$$\phi \sim \exp\left\{\pm ik[\omega^{-2}g(\Delta - \epsilon_1\sigma) - 1]^{1/2}z\right\} \qquad (10)$$

for $z \to -\infty$. In each case, the phase is defined by Eq. (9) & (10), and the solution having the positive sign has a downgoing phase while the solution having the negative sign has an upgoing phase. Upon referring to Fig. 3, we see that the vertical component of the energy flux is in the opposite direction, so the phase possessing the positive sign represents upgoing energy and that corresponding to the negative sign represents downgoing energy. A solution composed of a general linear combination of solutions of Eq. (6) will not, in general, solve the problem. This can best be seen by examining the mechanics of the reflection process. In the lower region, the solution (9) with positive sign represents the incoming wave with known amplitude and the solution (9) with negative sign is the reflected wave with unknown amplitude. In the upper region, however, there can be only the upgoing (transmitted) wave with unknown amplitude, so the solution (10) with negative sign should not be present.

The problem then reduces to predicting the amplitudes of the reflected and transmitted waves. This is a trivial task *only* if the anomalous region is reduced to zero thickness so that it can be replaced by an interface. In Appendix A, this classical case is compared with the solution obtained in the third section in the limit $\sigma \to \infty$. However, the particular Eq. (6) also is analytically tractable, and these wave amplitudes will be found in the analysis below. This work is comprised of the analytic continuation of the upgoing (negative sign) wave solution of expression (10) across the anomalous region into a linear sum of the solution (9). This continuation has been used by Epstein (8) for an equivalent problem in electromagnetic wave propagation. The analysis is redone here because the physical parameters enter the equations in a different way and because the present paper expands the problem to include a solution of the *general* case $\epsilon \neq 0$, $\epsilon_1 \neq 0$; furthermore, the solutions differ somewhat from those of Epstein (8).

Equation (6) may be rewritten in the form

$$\phi_{yy} + \left\{h^2 + \left(\frac{b}{4}\right)\operatorname{sech}^2\left(\frac{y}{2}\right) + c\tanh\left(\frac{y}{2}\right)\right\}\phi = 0, \tag{11}$$

where the change of variable

$$y = 2\sigma z \tag{12}$$

has been made and the parameters

$$\begin{aligned} h^2 &= \frac{\Delta g k^2}{4\sigma^2\omega^2} - \frac{k^2}{4\sigma^2} \\ b &= \frac{g\epsilon k^2}{\sigma\omega^2} \\ c &= \frac{g\epsilon_1 k^2}{4\sigma\omega^2} \end{aligned} \tag{13}$$

have been introduced. Another change of independent variable,

$$\xi = e^y, \tag{14}$$

transforms Eq. (11) to

$$\xi^2\phi_{\xi\xi} + \xi\phi_\xi + \left\{h^2 + b\xi(1+\xi)^{-2} + c(\xi-1)(\xi+1)^{-1}\right\}\phi = 0, \tag{15}$$

and the change of dependent variable

$$\phi = (1+\xi)^d\xi^a f, \tag{16}$$

where a and d are constants chosen below, yields the equation

$$\begin{aligned} &\xi(1+\xi)f_{\xi\xi} + [2a + 1 + (2a + 2d + 1)\xi]f_\xi + \Big\{2a + d \\ &+ [(a^2 + h^2)(1+\xi)^2 + d(d-1)\xi^2 + b\xi + c(\xi-1)(\xi+1)^{-1}] \\ &\times \xi^{-1}(1+\xi)^{-1}\Big\}f = 0. \end{aligned} \tag{17}$$

This equation may be reduced further if the constants a and b are chosen so that

$$\begin{aligned} a &= (c - h^2)^{1/2} \\ d &= \frac{1}{2} - \frac{1}{2}(1 + 4b)^{1/2}. \end{aligned} \tag{18}$$

With the final change of variable $\xi = -\zeta$, Eq. (17) reduces to Gauss' hypergeometric equation (13),

$$\zeta(1-\zeta)f_{\zeta\zeta} + [(2a+1) - (2a + 2d + 1)\zeta]f_\zeta - [(2a + d)d + 2c]f = 0. \tag{19}$$

In the region of the incident and reflected waves as $z \to \infty$ ($\xi \to \infty$), the solutions of Eq. (19) are (14),

$$\phi_1 \sim \xi^a(1+\xi)^d \xi^{-\alpha} F(\alpha, \alpha+1-\gamma; \alpha+1-\beta; (-\xi)^{-1})$$

$$\phi_2 \sim \xi^a(1+\xi)^d \xi^{-\beta} F(\beta, \beta+1-\gamma; \beta+1-\alpha; (-\xi)^{-1}) \tag{20a}$$

where $F(\ \ )$ represents the hypergeometric series and

$$\alpha = a + d + (a^2 - 2c)^{1/2}$$

$$\beta = a + d - (a^2 - 2c)^{1/2}$$

$$\gamma = 2a + 1. \tag{21}$$

The solutions in the far transmission region, as $z \to -\infty$ ($\xi \to 0$), are

$$\phi_3 \sim \xi^a(1+\xi)^d F(\alpha, \beta; \gamma; -\xi)$$

$$\phi_4 \sim \xi^a(1+\xi)^d(-\xi)^{1-\gamma} F(\alpha+1-\gamma, \beta+1-\gamma; 2-\gamma; -\xi). \tag{20b}$$

There are actually several ways in which the independent solutions (20a) and (20b) can be chosen; the forms above are selected for convenience in the following calculations.

With the aid of expressions (18) and (21), limiting forms of these solutions reduce to

$$\phi_1 \sim \exp\,[-2i(h^2+c)^{1/2}\sigma z]$$

$$\phi_2 \sim \exp\,[+2i(h^2+c)^{1/2}\sigma z] \tag{22a}$$

as $\xi \to \infty$ or $z \to \infty$, and

$$\phi_3 \sim \exp\,[2i(h^2-c)^{1/2}\sigma z]$$

$$\phi_4 \sim \exp\,[-2i(h^2-c)^{1/2}\sigma z] \tag{22b}$$

as $z \to -\infty$, in their respective regions of validity. As was discussed previously with respect to the solutions (9) and (10), ϕ_1 and ϕ_4 are downgoing waves (toward $z = +\infty$) and ϕ_2 and ϕ_3 are upgoing waves (toward $z = -\infty$) when viewed in terms of their group velocities. Thus, the limiting form of ϕ_3 as $z \to -\infty$ is a plane wave that transports energy *from* the anomalous region.

We therefore consider ϕ_3 as the wave transmitted through the anomalous layer; concommitantly, ϕ_4 is excluded from this role because its energy propagation direction is *toward* the anomalous layer. We remark that these asymptotic forms represent wavelike solutions only if $|c| < h^2$ or $|g\epsilon_1\sigma| < \alpha g - \omega^2$. This restriction in terms of wave propagation from the lower into the upper region is discussed on p. 18.

Since ϕ_3 represents the transmitted wave, this solution can be traced back through the layer. In the limit as $z \to \infty$, we will be able to represent ϕ_3 as a linear combination of ϕ_1 and ϕ_2. When the magnitude and phase of these complex coefficients are known, the total percentage of reflected and transmitted energy can be found. The process of

determining the representation of ϕ_3 in terms of ϕ_1 and ϕ_2 in their region of validity is called the analytic continuation of ϕ_3 into the region of validity of ϕ_1 and ϕ_2. A classical analytic continuation formula, valid for hypergeometric functions, is given by Erdélyi (14) as

$$F(\alpha, \beta; \gamma; -\xi) = \frac{\Gamma(\gamma)\Gamma(\beta-\alpha)}{\Gamma(\beta)\Gamma(\gamma-\alpha)}\,\xi^{-\alpha}F(\alpha, 1-\gamma+\alpha; 1-\beta+\alpha; (-\xi)^{-1}) + \frac{\Gamma(\gamma)\Gamma(\alpha-\beta)}{\Gamma(\alpha)\Gamma(\gamma-\beta)}\,\xi^{-\beta}F(\beta, 1-\gamma+\beta; 1-\alpha+\beta; (-\xi)^{-1}), \tag{23}$$

where $\Gamma(\ )$ represents the gamma function. Referring to expressions (20a) and (20b), we may employ this formula to express ϕ_3 as a linear combination of ϕ_1 and ϕ_2.

REFLECTION COEFFICIENT

The reflection coefficient, denoted by R, is defined as the coefficient of the reflected wave divided by the coefficient of the incident wave. The ratio of these amplitudes, however, is just the ratio of the coefficients in Eq. (23), so that

$$R = \frac{\Gamma(\beta-\alpha)\Gamma(\alpha)\Gamma(\gamma-\beta)}{\Gamma(\alpha-\beta)\Gamma(\beta)\Gamma(\gamma-\alpha)}\,. \tag{24}$$

As was noted in the second section, the amplitudes and phases of the transmitted and reflected waves differ from those of the incident wave. Since this amplitude and phase information is contained in each of the coefficients of Eq. (23), it is apparent that their ratio—the reflection coefficient—is a complex number. The amount of energy in an internal wave is proportional to the square of the wave amplitude, so the percentage of energy that is reflected is given by $100|R|^2$ where $|R|^2 = RR^*$. The total energy is conserved (to the Boussinesq approximation) under the assumptions in Eq. (2), so the percentage of energy transmitted is given by $100(1 - |R|^2)$.

Equation (24) contains the physical parameters associated with the thermocline scale height, density differences, and the horizontal wave number and direction of travel of the incident wave at $z = +\infty$. These are seen to enter in a rather complicated manner through the definitions of (13), (18), and (21), although Eq. (24) can be simplified to include only elementary functions of the physical parameters by limiting the discussion to $|R|^2$. The essential details of the reflection phenomenon can be obtained by plotting several special cases. In the next section, the solution for the *general* case of $\epsilon, \epsilon_1 \neq 0$ is given for a special restriction on the values ϵ and ϵ_1. The separate cases of the symmetrical layer ($\epsilon \neq 0$, $\epsilon_1 = 0$) and the transition layer ($\epsilon = 0$, $\epsilon_1 \neq 0$) are then treated in more detail.

General Case

For the *general* anomalous layer, $\epsilon, \epsilon_1 \neq 0$ with $b = g\epsilon k^2/\sigma\omega^2 \geqslant 1/4$, and the square of the magnitude of the reflection coefficient (24) is

$$|R|^2 = \left|\frac{\Gamma(\alpha)}{\Gamma(\beta)}\right|^2 \left|\frac{\Gamma(\beta-\alpha)}{\Gamma(\alpha-\beta)}\right|^2 \left|\frac{\Gamma(\gamma-\beta)}{\Gamma(\gamma-\alpha)}\right|^2 . \tag{25}$$

This expression is, in general, quite a complicated function of the physical parameters. We may, however, simplify Eq. (25) by considering the case for which $|c| < h^2$. The quantity $\alpha - \beta = 2(-h^2 - c)^{1/2}$ is then purely imaginary, so

$$\left|\frac{\Gamma(\beta-\alpha)}{\Gamma(\alpha-\beta)}\right|^2 = \left|\frac{\Gamma(-2[-h^2-c]^{1/2})}{\Gamma(2[-h^2-c]^{1/2})}\right|^2 = \left|\frac{\Gamma(z)}{\Gamma(z^*)}\right|^2 = 1.$$

Then, with the definitions of (21), Eq. (25) reduces to

$$|R|^2 = \left|\frac{\Gamma[a+d+(a^2-2c)^{1/2}]}{\Gamma[a+d-(a^2-2c)^{1/2}]}\right|^2 \left|\frac{\Gamma[1+a-d+(a^2-2c)^{1/2}]}{\Gamma[1+a-d-(a^2-2c)^{1/2}]}\right|^2 .$$

The identity

$$\Gamma(1-z) = \frac{\pi}{\Gamma(z)\sin \pi z}$$

permits further simplification of the above to

$$|R|^2 = \left|\frac{\Gamma[a+d+(a^2-2c)^{1/2}]}{\Gamma[-a+d-(a^2-2c)^{1/2}]}\right|^2 \left|\frac{\Gamma[d-a+(a^2-2c)^{1/2}]}{\Gamma[d+a-(a^2-2c)^{1/2}]}\right|^2$$

$$\times \left|\frac{\sin \pi\,[d-a+(a^2-2c)^{1/2}]}{\sin \pi\,[d-a-(a^2-2c)^{1/2}]}\right|^2 . \tag{26}$$

Now, the quantity $(a^2 - 2c)^{1/2}$ is imaginary for $|c| < h^2$, and d is real as long as $b > -1/4$ (the significance of this inequality is discussed below). If the discussion is restricted to this case, the first two terms in Eq. (26) are seen to be unity from the definition of the gamma function,

$$\Gamma(z) = \int_0^\infty e^{-t} t^{z-1} dt.$$

Finally, the last term can be expanded so that

$$|R|^2 = \frac{\sin^2 \pi d \cosh^2 \pi(b'-a') + \cos^2 \pi d \sinh^2 \pi(b'-a')}{\sin^2 \pi d \cosh^2 \pi(b'+a') + \cos^2 \pi d \sinh^2 \pi(b'+a')} , \tag{27}$$

where

$$b = \frac{g\epsilon k^2}{\sigma\omega^2} > -\frac{1}{4}$$

$$a' = (h^2 - c)^{1/2} = \left[\frac{\Delta g k^2}{4\sigma^2\omega^2} - \frac{k^2}{4\sigma^2} - \frac{g\epsilon_1 k^2}{\sigma\omega^2}\right]^{1/2}$$

$$b' = (h^2 + c)^{1/2} = \left[\frac{\Delta g k^2}{4\sigma^2\omega^2} - \frac{k^2}{4\sigma^2} + \frac{g\epsilon_1 k^2}{\sigma\omega^2}\right]^{1/2}$$

$$d = \frac{1}{2} - \frac{1}{2}(1 + 4b)^{1/2} = \frac{1}{2} - \frac{1}{2}\left[1 + \frac{4g\epsilon k^2}{\sigma\omega^2}\right]^{1/2}$$

$$|c| < h^2.$$

Equation (27) is the square of the reflection coefficient for a general combination of symmetrical and transitional layers of the form of Eq. (1) subject to the restrictions $b > -1/4$ and $|c| < h^2$. The physical implications of these inequalities are discussed in the following sections. The reflection coefficient is a function of three parameters, so further analysis will be limited to simpler cases.

Symmetrical Layer

In the case of the symmetrical layer, $\epsilon \neq 0$, $\epsilon_1 = 0$, $c = g\epsilon_1 k^2/4\sigma\omega^2 = 0$, and $b' = a' = h$; so, as long as $b \geqslant -1/4$, the reflection coefficient may be obtained from Eq. (27). It reduces to

$$|R|^2 = \frac{\sin^2 \pi d}{\sin^2 \pi d \cosh^2 2\pi h + \cos^2 \pi d \sinh^2 2\pi h}; \quad b \geqslant -\frac{1}{4}. \tag{28}$$

The case of $b < -1/4$ for the symmetrical layer must be treated separately. In this case,

$$d = \frac{1}{2} - \frac{i}{2}(1 - 4b)^{1/2} = \frac{1}{2} + id_2, \text{ say,}$$

and

$$a' = h,$$

so Eq. (24) reduces to

$$R = \frac{\Gamma\left[\frac{1}{2} + i(2h + d_2)\right]\Gamma(-2ih)\Gamma\left[\frac{1}{2} + i(2h - d_2)\right]}{\Gamma\left(\frac{1}{2} + id_2\right)\Gamma(2ih)\Gamma\left(\frac{1}{2} - id_2\right)}.$$

Use of the identity (Ref. 14)

$$\Gamma\left(\frac{1}{2} + id_2\right)\Gamma\left(\frac{1}{2} - id_2\right) = \frac{\pi}{\cosh \pi d_2}$$

allows a reduction of the above to

$$R = \frac{\Gamma(-2ih)}{\Gamma(2ih)} \frac{\cosh \pi d_2}{\pi} \Gamma\left[\frac{1}{2} + i(2h + d_2)\right] \Gamma\left[\frac{1}{2} + i(2h - d_2)\right].$$

We may now compute RR^* with the use of the identity

$$\Gamma\left(\frac{1}{2} - i\mu\right)\Gamma\left(\frac{1}{2} + i\mu\right) = \frac{\pi}{\sin \pi\left(\frac{1}{2} + i\mu\right)}.$$

The expression for RR^* is then seen to reduce to

$$RR^* = \frac{\cosh^2 \pi d_2}{\sin \pi\left[\frac{1}{2} + i(2h + d_2)\right] \sin \pi\left[\frac{1}{2} + i(2h + d_2)\right]}.$$

Or,

$$|R|^2 = \frac{\cosh^2 \pi d_2}{\cosh \pi [2h + d_2] \cosh \pi [2h - d_2]}, \qquad b < -\frac{1}{4}. \tag{29}$$

This formula, along with Eq. (28), completes the range of validity of the reflection coefficient for the symmetric layer ($\epsilon \neq 0$, $\epsilon_1 = 0$).

The two cases $b \gtrless -1/4$ must be treated separately merely for mathematical reasons. There is no apparent physical significance in the value of b being larger or smaller than -1/4. There are, however, *other* physical limitations on the value of b. In order that the Brunt-Väisälä frequency be nonnegative, b must satisfy the inequality

$$\frac{b}{4} + \frac{\Delta g k^2}{4\sigma^2 \omega^2} \geqslant 0$$

or, in the original variables,

$$\epsilon\sigma \geqslant -\Delta.$$

If ϵ were a larger negative than this, the basic state would be statically unstable in the neighborhood of $z = 0$ (see Fig. 2). Another range of the variable b that is of interest is seen to be when b is a sufficiently large negative number so that

$$\frac{b}{4} + h^2 \leqslant 0.$$

In the original variables, this implies that

$$g\epsilon\sigma \leqslant -(\Delta g - \omega^2).$$

In this case, the upward-propagating wave encounters an evanescent layer in the neighborhood of $z = 0$. That is, the propagation constant (or restoring force) in Eq. (6) is negative and solutions of the equation are locally monotonic instead of oscillatory. If this occurs over a sufficiently large vertical region, one would expect that most of the wave energy would be reflected.

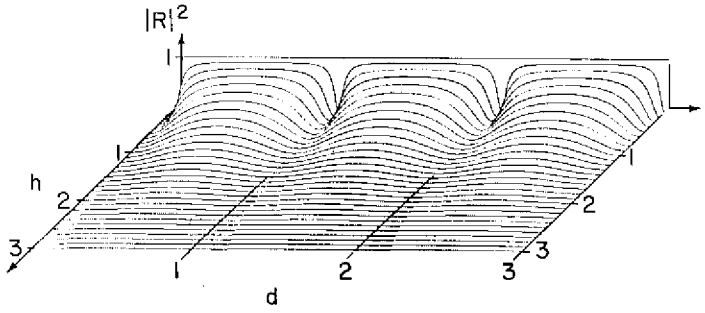

Fig. 4a—The logarithm of the square of reflection coefficient (log $|R|^2$) for a symmetric layer. Log $|R|^2$ is plotted as a function of d and h.

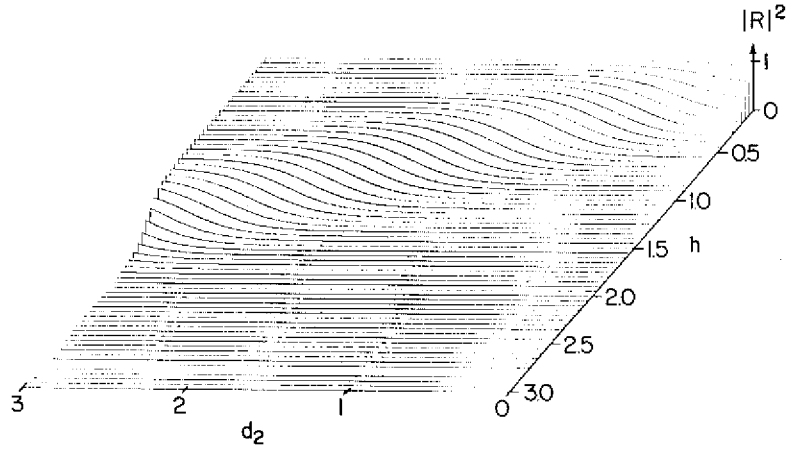

Fig. 4b—Log $|R|^2$ as a function of d_2 and h.

Equations (28) and (29) contain only two parameters, so that their significance is relatively easy to appreciate. Figure 4 shows plots of the reflection coefficients as functions of the two parameters d and h. These graphs can therefore be used to obtain the reflection coefficient for any particular *combination* of the physical variables in the case of the symmetric layer. It is also instructive to illustrate the functional dependence of $|R|^2$ upon the individual parameters in definitions (13). Specifically, these are $k\sigma^{-1}$, the

ratio of the horizontal wave number to the scale length of the layer, and θ, the angle of the incident wave with respect to the horizontal. Figure 5 shows several plots graphed on

Symbols for $k\sigma^{-1}$ for 5a., 5b., 5c.

◇ = 0.005	× = 0.25
+ = 0.01	△ = 0.50
⬡ = 0.05	⊡ = 1.0
⊙ = 0.1	▽ = 5.0

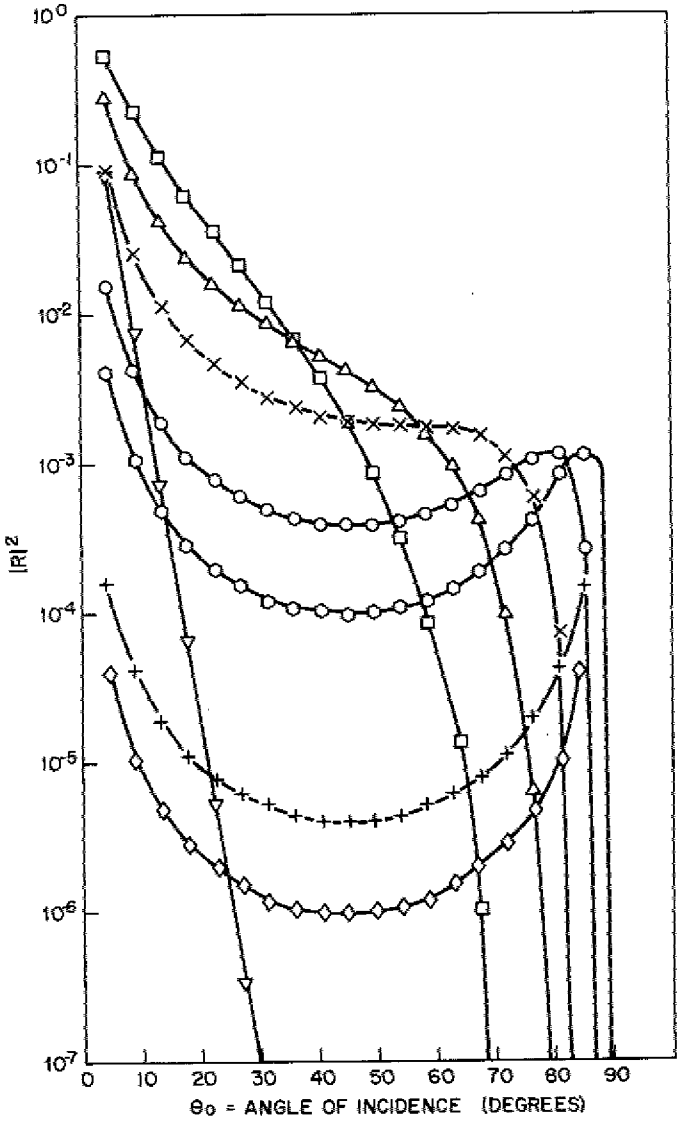

Fig. 5a—Log $|R|^2$ as a function of θ and $k\sigma^{-1}$; $\frac{N^2_{max}}{N^2_{min}} - 1 = 0.1$

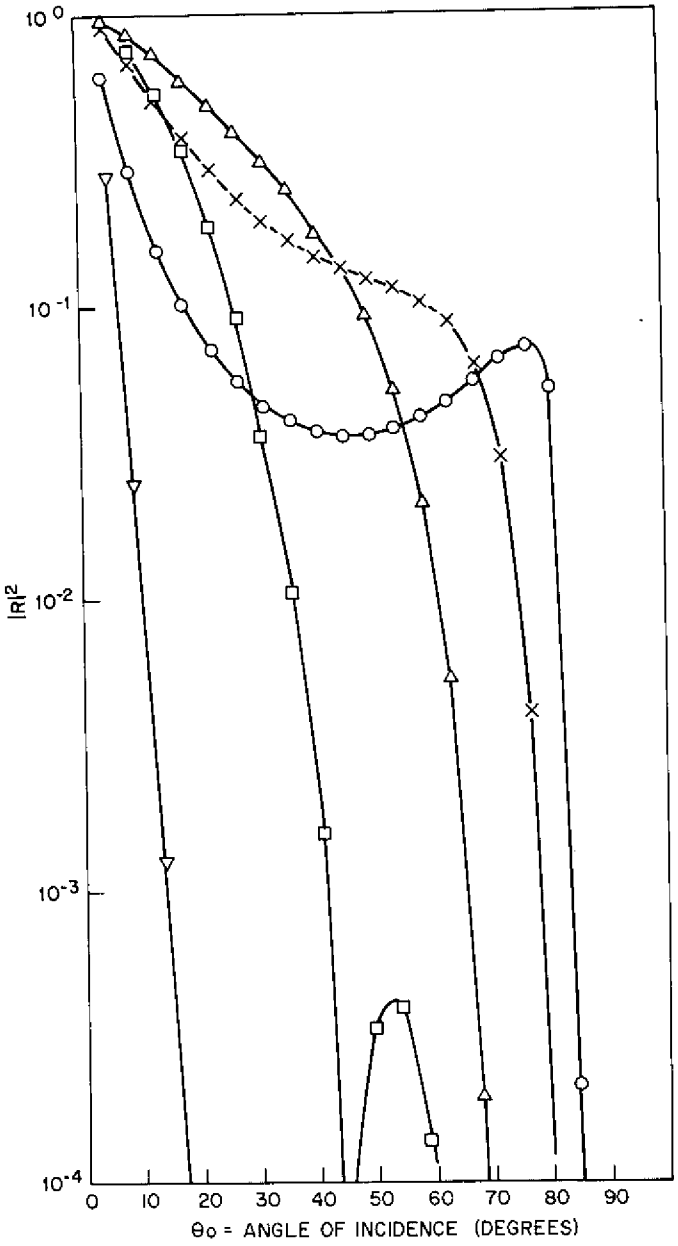

Fig. 5b—Log $|R|^2$ as a function of θ and $k\sigma^{-1}$; $\frac{N_{max}^2}{N_{min}^2} - 1 = 1.0$

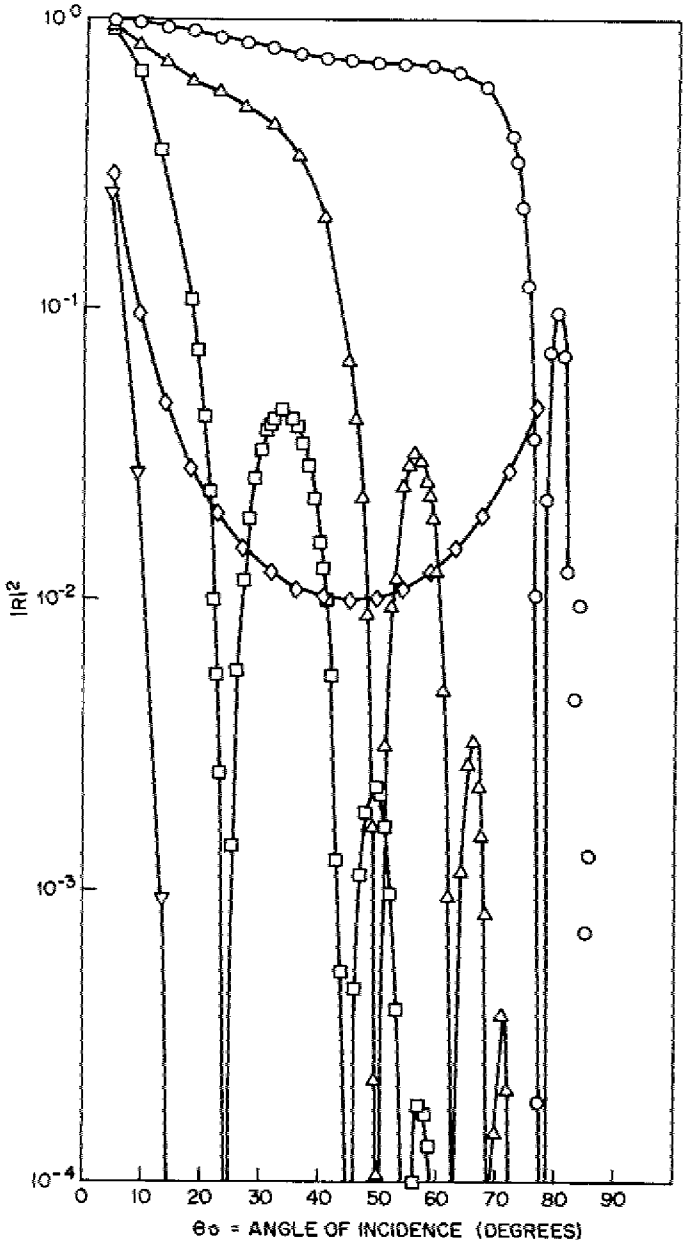

Fig. 5c—Log $|R|^2$ as a function of θ and ka^{-1}; $\frac{N^2_{max}}{N^2_{min}} - 1 = 10.0$

a logarithmic scale to enhance the appearance of windows at high angles of incidence. To further illustrate this phenomenon, a surface of $|R|^2$ is plotted vs θ and $k\sigma^{-1}$ in Fig. 6 for several values of $(\epsilon\sigma/\Delta) - 1$. If $|R|^2 < 10^{-3}$, $|R|^2 \equiv 10^{-3}$ here and *et seq.*

The dependence of the reflection coefficient upon the physical parameters is rather complicated despite the deceivingly simple appearance of Eqs. (28) and (29). There are several interesting observations that can be made, however. First, the reflection coefficient is always unity for waves traveling horizontally and always vanishes for those traveling vertically. The former limit occurs because a wave with horizontal phase speed consists of vertical columns of water moving up and down alternately. The density anomaly at the pycnocline, no matter how small, is not easily displaced by the wave. As the size of the density anomaly $O(1/\sigma)$ increases with respect to the vertical wavelength $O(k \tan \theta)^{-1}$, the dependence of the reflection coefficient is more complicated. Multiple windows occur for which practically all of the energy passes through the layer. As θ increases to 90°, the vertical wavelength decreases to zero, so that more and more wavelengths are compressed into the layer; hence, these windows tend to accumulate in the vicinity of $\theta = 90°$. The appearance of the windows is a little surprising, but the fact that an envelope of the reflection coefficient goes to zero as θ approaches 90° is not. The vertical wavelength becomes short compared to the length scale of the density anomaly, so the classical WKB approximation becomes valid. It is well known that the WKB solution does not allow reflection unless the wave encounters an evanescent region.

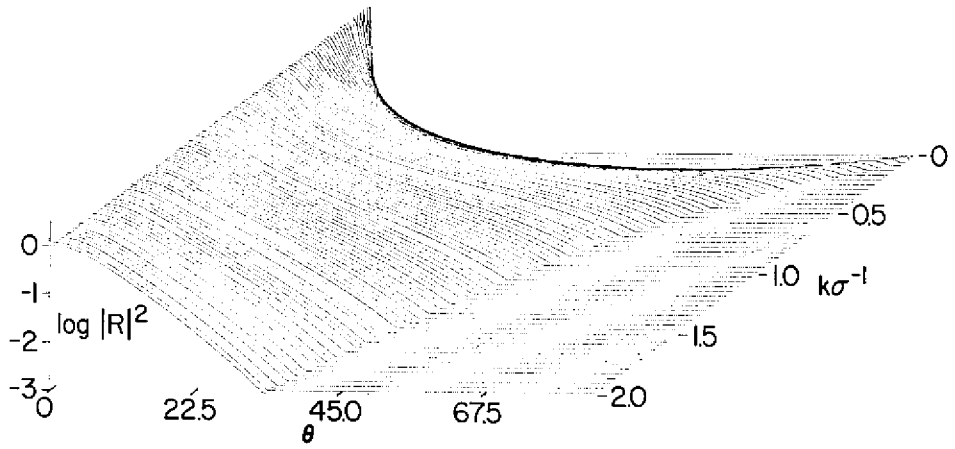

Fig. 6a—Log $|R|^2$ vs θ and $k\sigma^{-1}$ for $\frac{\epsilon\sigma}{\Delta} - 1 = 0.1$

The limit of $k\sigma^{-1} \to 0$ is a peculiar one in this case, and it is discussed in Appendix A.

Transitional Layer

This is the case in which $\epsilon = 0$, $\epsilon_1 \neq 0$. Proceeding to evaluate the reflection coefficient in expression (24) in this case, we see that there are two fundamentally different cases (see Fig. 2b);

1. $\epsilon_1 > 0$ and $c \geqslant h^2$ (30)
2. $\epsilon_1 > 0$ or $\epsilon_1 < 0$ and $|c| \leqslant h^2$. (31)

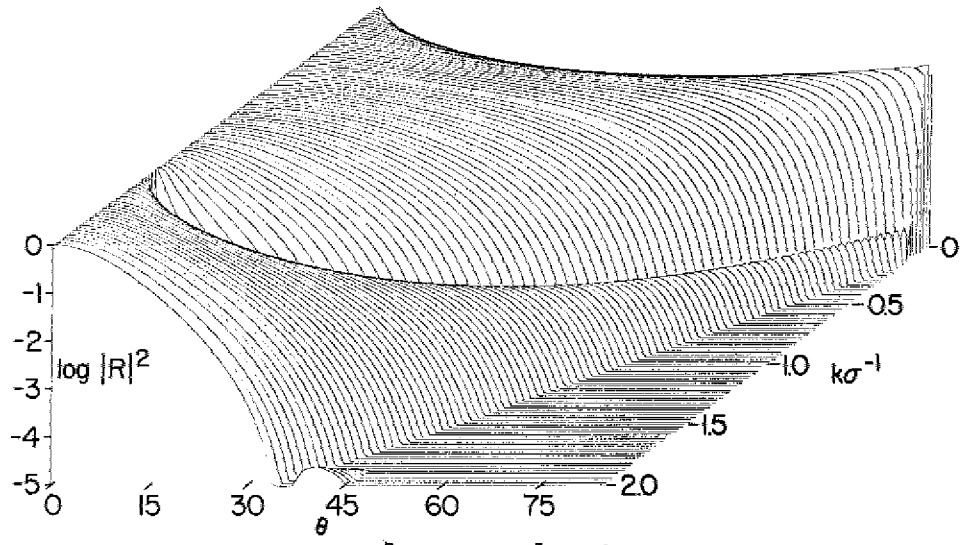

Fig. 6b—Log $|R|^2$ vs θ and $k\sigma^{-1}$ for $\frac{\epsilon\sigma}{\Delta} - 1 = 1.0$

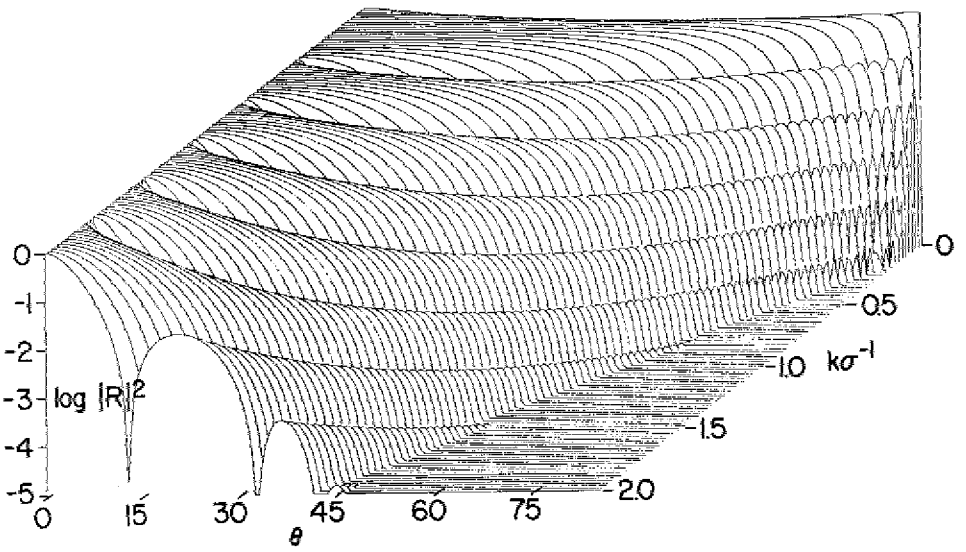

Fig. 6c—Log $|R|^2$ vs θ and $k\sigma^{-1}$ for $\frac{\epsilon\sigma}{\Delta} - 1 = 10.0$

In each of these cases, the form of the reflection coefficient changes; this corresponds to different propagation conditions. Because of the physical significance of these, we shall explore each one separately below.

Case 1. In this instance, $\epsilon_1 > 0$ and the region of higher Brunt-Väisälä frequency occupies the lower half-plane. The inequality $c \geqslant h^2$ implies that $g(\Delta - \epsilon_1\sigma) \leqslant \omega^2 \leqslant g(\Delta + \epsilon_1\sigma)$. Since the frequency of the transmitted wave is ω, we expect that the squar of this frequency would be less than $g(\Delta - \epsilon_1\sigma)$ for there to be wave propagation in the upper layer. In the inequality above, we see that these values of ω^2 are not allowed. One would expect, therefore, that a wave incident on this thermocline at any angle from below would be totally reflected. In fact, if $c \geqslant h^2$, we see that

$$\alpha = \delta_1 + i\delta_2$$

$$\beta = \delta_1 - i\delta_2$$

and

$$\gamma = 2\delta_1 + 1.$$

The real quantities δ_1 and δ_2 are defined by

$$c - h^2 = \delta_1^2$$

and

$$c + h^2 = + \delta_2^2, \qquad \delta_1 \geqslant 0.$$

Then,

$$R = \frac{\Gamma(-2i\delta_2)\Gamma(\delta_1 + i\delta_2)\Gamma(\delta_1 + 1 + i\delta_2)}{\Gamma(2i\delta_2)\Gamma(\delta_1 - i\delta_2)\Gamma(\delta_1 + 1 - i\delta_2)}$$

and

$$|R|^2 = 1. \tag{32}$$

We see that all energy indeed is reflected in the case $\epsilon_1 > 0$ and that $g(\Delta - \epsilon_1\sigma) \leqslant \omega^2 \leqslant g(\Delta + \epsilon_1\sigma)$, as we anticipated above.

Case 2. Here, we may have ϵ_1 again greater than zero, but $\epsilon_1 < 0$ is also allowed and $|c| < h^2$. From our discussion in the second section on the conditions under which internal waves will propagate, we would expect that at least a portion of the wave energy would be transmitted up through the transition regions. If $\epsilon_1 > 0$, $\omega^2 < g(\Delta - \epsilon_1\sigma)$; and, if $\epsilon_1 < 0$, $\omega^2 < g(\Delta + \epsilon_1\sigma)$. Both of these conditions will allow at least partial transmission through the anomalous region. Using the above definitions of δ_1 and δ_2, we have

$$\alpha = i\delta_2 + i\delta_1,$$

$$\beta = i\delta_1 - i\delta_2,$$

and

$$\gamma = 1 + 2\delta_1.$$

Using these quantities in Eq. (24), we may calculate RR^* with the use of the identities (Ref. 15)

$$\Gamma(i\mu)\Gamma(-i\mu) = \frac{\pi}{\mu \sinh \pi\mu}$$

and

$$\Gamma(1 + i\mu)\Gamma(1 - i\mu) = \frac{\pi\mu}{\sinh \pi\mu} .$$

Then,

$$|R|^2 = \frac{\sinh^2 \pi(\delta_1 - \delta_2)}{\sinh^2 \pi(\delta_1 + \delta_2)} . \tag{33}$$

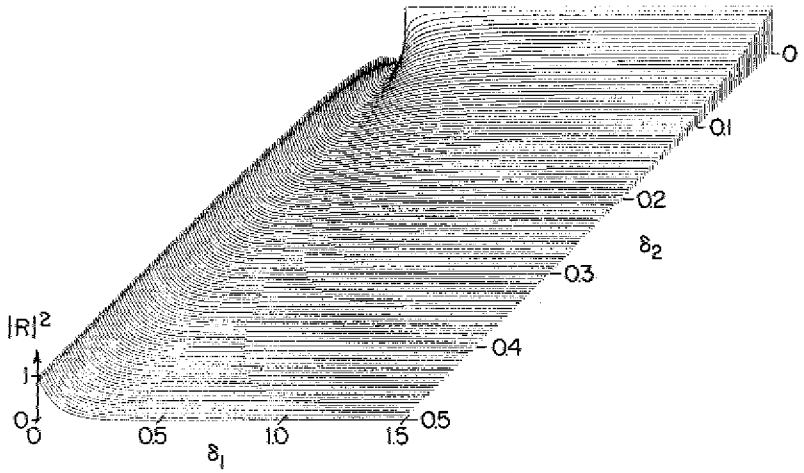

Fig. 7—Log $|R|^2$ for the transition layer ($\epsilon_1 \gtrless 0$, $\epsilon = 0$) as a function of δ_1 and δ_2. Case 2.

A graph of this expression appears in Fig. 7 as a function of δ_1 and δ_2. This result is interesting in that it is independent of the sign of the parameter ϵ_1—that is, the reflection mechanism does not depend upon whether the waves are going from less stable to more stable fluid, or vice versa. Expressed in the original physical parameters however, the value of $|R|^2$ *is* dependent upon $sgn(\epsilon_1)$ because the angle of incidence is a function of ϵ_1.

It is of interest to consider the special case $k\sigma^{-1} \tan\theta \to 0$; that is, the limit in which the transition layer is thin compared to the vertical wavelength of the internal wave. The parameters δ_1 and δ_2 are linear functions of $k\sigma^{-1}$, so the hyperbolic functions can be replaced by their arguments in the limit $k\sigma^{-1} \to 0$ to yield

$$|R| = \frac{\delta_1 - \delta_2}{\delta_1 + \delta_2} . \tag{34}$$

Although δ_1 and δ_2 remain complicated functions of the physical parameters, this is simply a Fresnel reflection formula. It is shown in Appendix A that the reflection coefficient for a two-layer fluid in which the layers are separated by a jump discontinuity in $N^2(z)$ gives the same results.

CONCLUSIONS

In the second section, it was shown that the equation governing the z-dependent part of the vertical velocity may be transformed to the hypergeometric equation. The existence of analytic continuation formulae for this equation allows a solution representing a plane wave in the upper half-space above the pycnocline to be expressed as a linear, complex sum of two plane waves in the region far below the pycnocline. To correspond with the physically motivated problem of barrier transmission, we have chosen the phases of the three waves so that the solution above the thermocline represents a wave with group velocity away from the thermocline—the transmitted wave. The two waves below the pycnocline are the waves incident on, and reflected by, the variation in density.

As was discussed in the third section, the reflection coefficient R is actually a complex number containing information on the phase and amplitude of the reflected wave relative to those of the incident wave. We have shown that a general thermocline form—one which is a combination transition region and symmetric layer—possesses a reflection coefficient expressible in terms of gamma functions having arguments which are functions of θ, $k\sigma^{-1}$, ϵ, and ϵ_1. For a particular range of the parameter $b > -1/4$ (where $b = g\epsilon k^2/\sigma\omega^2$), the solution may be considerably simplified when $\omega^2 < g(\Delta - |\epsilon_1|\sigma)$, and it is given by expression (27). This form of $|R|^2$ is a function of the parameters h, b, and c (see Eqs. (13)).

To better exhibit the behavior of $|R|^2$ as a function of the physical parameters, we alternately equate ϵ and then ϵ_1 to zero. The former case is that of the symmetrical layer which may also serve as a waveguide for horizontally propagating waves, while the latter case is that of the transition layer (see Fig. 2).

The reflection coefficient for the symmetric layer is shown in Fig. 4. It is comprised of two graphs of $|R|^2$ for the values $b > -1/4$ and $b < -1/4$. As discussed previously, there appears to be no physical significance to the value $b = -1/4$. Although the form of the solution changes in the two ranges of b, it is continuous at this value of b.

No striking behavior in $|R|^2$ is apparent in these graphs. A plot of the square of the reflection coefficient as a function of θ for the symmetrical layer is given in Fig. 5 for various values of $k\sigma^{-1}$. The behavior of $|R|^2$ appears to be a rather complicated function of $k\sigma^{-1}$. To exhibit this dependence more carefully, an isometric plot of log $|R|^2$ is given in Fig. 6 for the parameter $(g\epsilon_1\sigma/g\Delta) - 1$ equal to 0.1, 1.0 and 10.0. Values of $|R|^2$ are arbitrarily equated to zero when they are smaller than the lowest ordinate given. The behavior of $|R|^2$ is now quite apparent. At low values of the parameter $(g\epsilon_1\sigma/g\Delta) - 1$, equal to 0.1, say, there is one hump or tunnel passing from values of large $k\sigma^{-1}$ and small θ to values of large θ and small $k\sigma^{-1}$. For small $k\sigma^{-1}$, the troughlike behavior of $|R|^2$ present in Fig. 5 is apparent in the isometric plot (Fig. 6). When the parameter equals 1.0, Fig. 5 reveals a complicated oscillatory behavior in $|R|^2$. We see here that the "windows" discussed briefly on p. 17 start to appear and become more numerous as the parameter becomes larger, for example, of order 10.0. As θ approaches 90°, the windows seem to accumulate and we conjecture that the explanation is as follows. For wave numbers inclined progressively more toward the vertical, the vertical wave number becomes large, tending toward infinity as $\theta \to 90°$. In this limiting process, many wavelengths are able to fit into a region the order of the thermocline thickness $O(1/\sigma)$. A small change in θ, therefore, can result in a significantly larger or smaller number of such contained wavelengths. Since the process of reflection is one of constructive or destructive interference of these waves, the windows would then be expected to accumulate in the region $\theta \simeq 90°$.

The plot of the transition layer reflection coefficient appears in Fig. 7. As was discussed on p. 18, when $\epsilon_1 > 0$ but $g(\Delta - \epsilon_1\sigma) \leqslant \omega^2 \leqslant g(\Delta + \epsilon_1\sigma)$, a wave of frequency ω incident from below cannot propagate into the upper region. All of the energy is reflected; none is transmitted, and $|R|^2 = 1$. On the other hand, the case for which $\epsilon_1 \gtrless 0$ and $\omega^2 < g(\Delta - |\epsilon_1|\sigma)$ exhibits incomplete reflection, and a plot of $|R|^2$ as a function of δ_1 and δ_2 appears in Fig. 7. The behavior is deceivingly simple, with $|R|^2$ being asymptotic to a constant for large values of δ_1 or δ_2. The variables δ_1 and δ_2 are somewhat more complicated functions of θ, $k\sigma^{-1}$ and ϵ_1. As such, their significance is not readily appreciated from a simple plot of the type shown in Fig. 7. Another plot of $|R|^2$ is shown in Fig. 8 as a function of $k\sigma^{-1}$ and θ. This figure shows the reflection coefficient as a function of θ and $k\sigma^{-1}$ for several different values of $g\epsilon_1\sigma/\omega^2$: 2, 10, and 50. $|R|^2$ appears to change very little for these widely spaced values of $g\epsilon_1\sigma/\omega^2$; the only alteration in appearance seems to be a tendency toward higher reflection coefficients for larger θ as $g\epsilon_1\sigma/\omega^2$ becomes large.

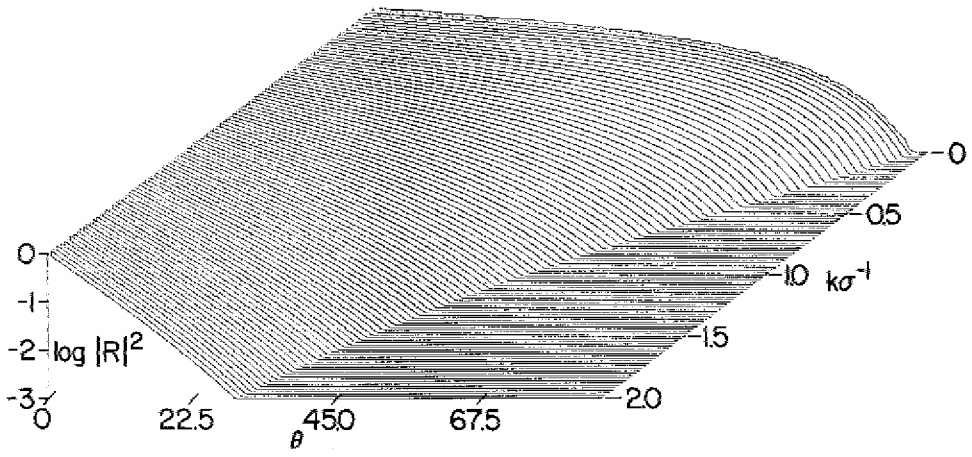

Fig. 8a—Log $|R|^2$ for the transition layer ($\epsilon = 0$) vs θ and $k\sigma^{-1}$ for $2g\epsilon_1/\omega^2 = 4.0$ and $\epsilon_1 > 0$.

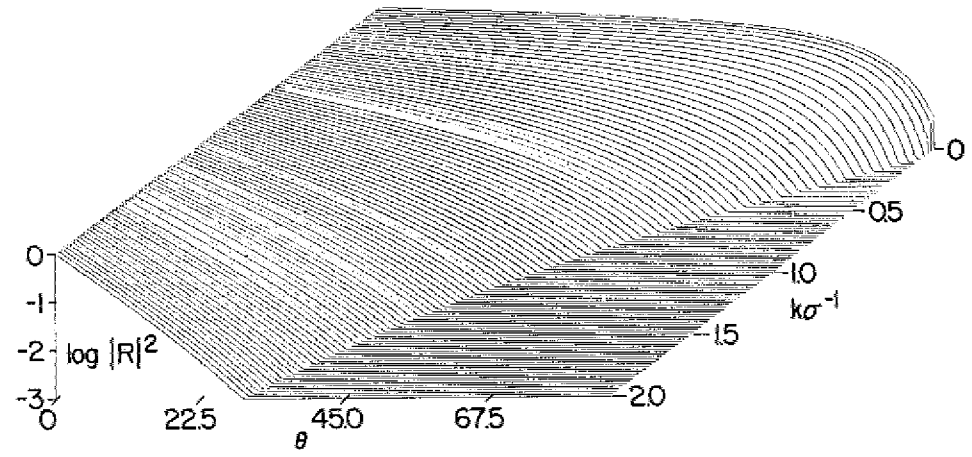

Fig. 8b—Log $|R|^2$ for the transition layer ($\epsilon = 0$) vs θ and $k\sigma^{-1}$ for $2g\epsilon_1/\omega^2 = 20.0$ and $\epsilon_1 > 0$.

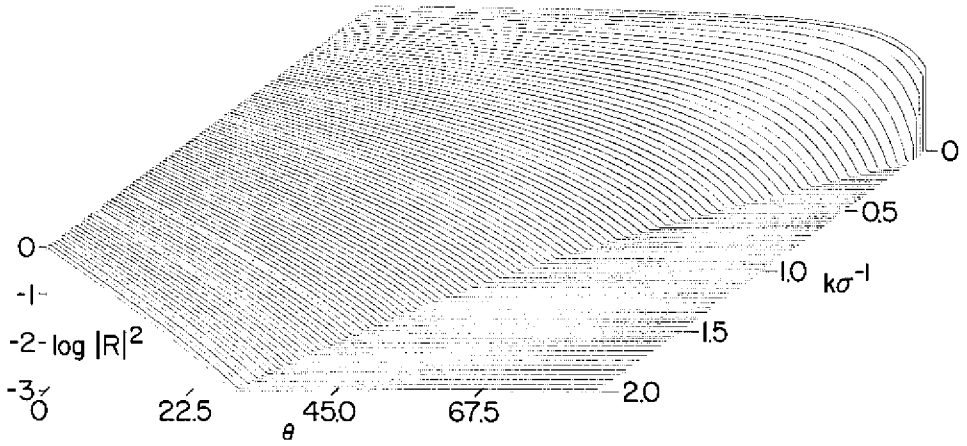

Fig. 8c—Log $|R|^2$ for the transition layer ($\epsilon = 0$) vs θ and $k\sigma^{-1}$ for $2g\epsilon_1/\omega^2 = 100.0$ and $\epsilon_1 > 0$.

Although the dependence of $|R|^2$ on physical parameters in either the symmetric or transition cases is quite varied depending upon the values of the physical parameters, we may draw a number of general conclusions. When the phase speed of the incident wave is horizontal ($\theta = 0°$), the group velocity is vertical (see, e.g., Phillips, Ref. 11) and the wave motion consists of vertically oscillating columns of fluid. In this case, all of the wave energy is reflected. On the other hand, waves for which $\theta = 90°$ have vertically directed wave numbers but zero frequency. Their group velocity is therefore zero, and we find that $|R|^2 \to 0$, although perhaps not monotonically because of the possible presence of the windows. The behavior $|R|^2 \to 0$ as $\theta \to 90°$ is, in a sense, a degenerate one because zero-frequency waves do not propagate. They reduce to a steady, horizontal current. Since the group velocity vanishes, the question of reflection or transmission of that energy is an inappropriate one.

Although the pycnoclines discussed in this report represent a specialized physical situation, the advantage in their treatment is that the parametric behavior of $|R|^2$ may be examined as certain physical parameters are changed. In Appendix B, a method for treating reflection from general pycnoclines is discussed. This subject will be dealt with in more detail in another report.

REFERENCES

1. J. W. Miles, "Waves and Wave Drag in Stratified Flows," *Applied Mechanics:* Proc. 12th Intl. Cong. Applied Mechanics. (M. Hetényi and W. G. Vincenti, eds.) Springer-Verlag, Berlin, 1969, pp 50-76.

2. R. Kh. Zeytounian, Phénomènes d'ondes dans les écoulements stationnaries d'un fluide stratifié non visqueux. I. Modèles théoriques. *J. de Mécanique* 8, 239-263 (1969).

3. R. Kh. Zeytounian, Phénomènes d' ondes dans les écoulements stationnaries d'un fluide stratifié non visqueux. II. Applications météorologiques: ondes de relief dans une atmosphère barocline. *J. de Mécanique* 8, 335-355 (1969).

4. J. R. Booker, and F. P. Bretherton, "The Critical Layer for Internal Gravity Waves in a Shear Flow," *J. Fluid Mech.* 27, 513 (1967).

5. R. J. Breeding, "A Non-linear Investigation of Critical Levels for Internal Atmospheric Gravity Waves," *J. Fluid Mech.* 50 (3) 545 (1971).

6. C. O. Hines, and C. A. Reddy, "On the Propagation of Atmospheric Gravity Waves through Regions of Wind Shear," *J. Geophys. Res.* 72 (3), 1015-1034 (1967).

7. A. Barcilon, S. Blumsack, and J. Lau, "Reflection of Internal Gravity Waves by Small Scale Density Variations," *J. Phys. Ocean.* 2 (1), 104-107 (1971).

8. P. S. Epstein, "Reflection of Waves in an Inhomogeneous Absorbing Medium," *Proc. Natl. Acad. Sci.* 16 (10), 627 (1930).

9. C. Iselin, "A study of the Circulation of the Western North Atlantic," *Phys. Ocean. Meteor.* 6 (4) (1936).

10. J. D. Woods, "Wave-Induced Shear Instability in the Summer Thermocline," *J. Fluid Mech.* 32 (4), pp 791-800 (1968).

11. O. M. Phillips, Ch. 5 in *The Dynamics of the Upper Ocean* Cambridge University Press, Cambridge, England, 1966.

12. I. Orlanski and K. Bryan, "Formation of the Thermocline Step Structure by Large-Amplitude Internal Gravity Waves," *J. Geophys. Res.* 74 (28), 6975-6983 (1969).

13. E. T. Whittaker and G. N. Watson, *A Course of Modern Analysis*, Cambridge University Press, Cambridge, England, 1963, p 283.

14. A. Erdélyi, ed. *Higher Transcendental Functions*, Vol. 1, McGraw-Hill, New York, 1953.

15. M. Abramowitz and I. Stegun, *Handbook of Mathematical Functions*, Dover, New York, 1965, p 256.

Appendix A
REFLECTION FROM A THIN DENSITY ANOMALY

In the special case where a layered density anomaly is very thin in comparison to the vertical wavelength of the internal wave, the reflection problem becomes much simpler to solve. The anomalous region may be reduced, at least in the limit, to a line so that the layer is replaced by an appropriate boundary condition.

We treat the two cases shown in Fig. A1. Case I is the limit of a symmetrical stable layer, and Case II is the limit of a transition layer. In each case, the solutions in the upper and lower layers are plane-propagating waves. The solutions for the vertical velocity components in the waves are

$$\begin{aligned} w_{in} &= \exp\left\{i[kx - n_\ell z - \omega t]\right\} \\ w_{re} &= -R \exp\left\{i[kx + n_\ell z - \omega t]\right\} \\ w_{tr} &= T \exp\left\{i[kx - n_u z - \omega t]\right\}, \end{aligned} \tag{A1}$$

where w_{in}, w_{re}, and w_{tr} represent the incoming, reflected, and transmitted waves. The constants R and T are the amplitudes of the reflected and transmitted waves, and n_ℓ and n_u are the vertical wavenumbers of the waves in the lower and upper regions, respectively.

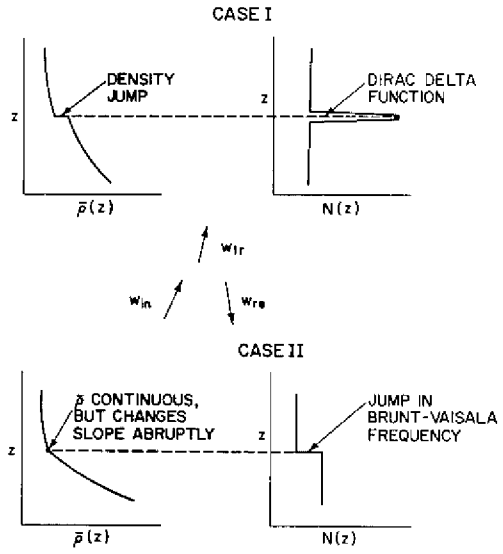

Fig. A1—Plots of $\bar{\rho}(z)$ and $N(z)$ for Case I and II.

The boundary conditions to be satisfied at the interface between the two layers are that the vertical velocity and the pressure are continuous there. In terms of the vertical velocity, these reduce to

$$[w] = 0$$

$$[\bar{\rho} w'] = \frac{gk^2}{\omega^2} [\bar{\rho}] w, \tag{A2}$$

where the brackets [ ] represent the difference between the values on the two sides of the interface*. In Case I, to the Boussinesq approximation, the reflection coefficient is

$$|R| = \frac{1}{1 + \dfrac{2\rho_{av}(N_0^2\omega^2 - \omega_4)^{1/2}}{gk\Delta\rho}} , \tag{A3}$$

where ρ_{av} is the average density on the two sides of the interface and $\Delta\rho$ is the density difference. In Case II, the reflection coefficient is

$$|R| = \frac{n_u - n_\ell}{n_u + n_\ell} . \tag{A4}$$

The latter solution agrees with the reflection coefficient of Eq. (34) that is the limit as the transition region shrinks to zero. This special case serves as a check on the results obtained for the transition region.

On the other hand, the solution Eq. (A3) is *not* the same as the limiting value of expression (28) as the symmetrical layer shrinks to zero. This should not be surprising, since this limit is the same as placing a delta function in a coefficient of the governing equation,

$$\phi_{zz} + k^2 \left\{\omega^{-2} g[\Delta + \epsilon\sigma \operatorname{sech}^2 \sigma z + \epsilon_1 \sigma \tanh \sigma z] - 1\right\} \phi = 0 \tag{A5}$$

or

$$\phi_{zz} + \left[\frac{N^2(z)}{\omega^2} - 1\right] k^2 \phi = 0. \tag{A6}$$

The difference in the results is caused entirely by reversing the order in which a limit is taken. In the continuous profile examined in the body of the report, the limit of $k\sigma^{-1} \to 0$ is taken of the solution of the governing equation (A6). In this appendix, the reflection coefficient is obtained from the solution of the equation resulting from the limit of the governing equation (A6).

We suggest that in the limit of $k\sigma^{-1} \to 0$, the reflection coefficient (A3) is more reliable than the appropriate limit of the expression

*C.S. Yih, *Dynamics of Nonhomogeneous Fluids*, New York, Macmillan, 1965, p. 21.

$$|R|^2 = \frac{\sin^2 \pi d}{\sin^2 \pi d \cosh^2 2\pi h + \cos^2 \pi d \sinh^2 2\pi h} \quad ; \quad b > \frac{1}{4} .$$

This choice is a simple one. The limiting solution of Eq. (A6) has a very large number of oscillations in the small anomalous region, so that the solution is not physically realistic.

Appendix B
A NUMERICAL METHOD FOR FINDING REFLECTION COEFFICIENTS FOR ARBITRARY BRUNT-VÄISÄLÄ DISTRIBUTIONS

In virtually all wave reflection problems of physical interest, it is impossible to model the pycnocline with an analytical expression. It is therefore of interest to devise a method which gives accurate reflection coefficients without resorting to layer modeling.

An acceptable method of solution is then as follows. Given a transmitted wave with upward group velocity,

$$w \sim \exp\{i(kx - nz - \omega t)\}$$

as an initial condition, we may integrate the equation

$$w'' + \left(\frac{N^2}{\omega^2} - 1\right) k^2 w = 0$$

from $z = -\infty$ *backward* through the pycnocline into the region of constant Brunt-Väisälä frequency below. The solution in the vicinity of $z = +\infty$ is then a linear sum of two waves, the incident and the reflected wave. By making use of the phase and amplitude of the solution near $z = +\infty$ with respect to those of the solution near $z = -\infty$, we may calculate a value of $|R|^2$. To check the accuracy of the method, a test case was tried. The reflection coefficient for a wave with

$$N^2 = g\Delta + g\epsilon\sigma \operatorname{sech}^2 \sigma z$$

was calculated for $k\sigma^{-1} = 1$, $\theta = 22.5°$, and $g\epsilon\sigma/g\Delta - 1 = 1$. The numerical integration technique was found to give an answer in error of the true value ($|R|^2 = 0.1897$) by 10^{-3}. A thorough treatment of this method will appear in a later work.